Reisler, E., Burke, M., & Harrington, W. F. (1974) *Biochemistry 13*, 2014-2022.
Schaub, M. C., Watterson, J. G., & Wasser, P. G. (1975) *Hoppe-Seyler's Z. Physiol. Chem. 356*, 325-339.
Seidel, J. C. (1969) *Biochim. Biophys. Acta 180*, 216-219.
Seidel, J. C., & Gergely, J. (1971) *Biochem. Biophys. Res. Commun. 44*, 826-830.
Sekine, T., & Kielley, W. W. (1964) *Biochim. Biophys. Acta 81*, 336-345.
Sleep, J. A., & Taylor, E. W. (1976) *Biochemistry 15*, 5813-5817.
Stein, L. A., Schwarz, R. P., Jr., Chock, P. B., & Eisenberg, E. (1979) *Biochemistry 18*, 3895-3909.
Sutoh, K., & Hiratsuka, T. (1988) *Biochemistry 27*, 2964-2969.
Suzuki, R., Nishi, N., Tokura, S., & Morita, F. (1987) *J. Biol. Chem. 262*, 11410-11412.
Toyoshima, Y. Y., Kron, S. J., McNally, E. M., Niebling, K. R., Toyoshima, C., & Spudich, J. A. (1987) *Nature 328*, 536-539.
Ue, K. (1987) *Biochemistry 26*, 1889-1894.
Walker, J. E., Saraste, M., Runswick, M. J., & Gay, N. J. (1982) *EMBO J. 1*, 945-951.
Weeds, A. G., & Taylor, R. S. (1975) *Nature 257*, 54-56.
Wells, J. A., & Yount, R. G. (1979) *Proc. Natl. Acad. Sci. U.S.A. 76*, 4966-4970.
Wells, J. A., & Yount, R. G. (1980) *Biochemistry 19*, 1711-1717.
Wells, J. A., Knoeber, C., Sheldon, M. C., Werber, M. M., & Yount, R. G. (1980) *J. Biol. Chem. 255*, 11135-11140.
Werber, M. M., Szent-Gyorgyi, A. G., & Fasman, G. D. (1972) *Biochemistry 11*, 2872-2882.
Yamaguchi, M., & Sekine, T. (1966) *J. Biochem. (Tokyo) 59*, 24-33.

The Rigor Configuration of Smooth Muscle Heavy Meromyosin Trapped by a Zero-Length Cross-Linker†

Hirofumi Onishi* and Keigi Fujiwara

Department of Structural Analysis, National Cardiovascular Center Research Institute, Fujishiro-dai, Suita, Osaka 565, Japan

Received September 8, 1989; Revised Manuscript Received November 9, 1989

ABSTRACT: When chicken gizzard heavy meromyosin (HMM) in its rigor complex with actin was reacted with the zero-length cross-linker 1-ethyl-3-[3-(dimethylamino)propyl]carbodiimide (EDC), HMM cross-linked with actin but also the two heads of the HMM molecule cross-linked to each other [Onishi, H., Maita, T., Matsuda, G., & Fujiwara, K. (1989) *Biochemistry 28*, 1898-1904, 1905-1912]. By ultracentrifugal fractionation of the EDC-treated acto–HMM in the presence of Mg-ATP, we obtained a preparation enriched for gizzard HMM with cross-linked heads. When HMM molecules in this preparation were rotary-shadowed and observed in an electron microscope, many head pairs were in contact with each other. The amount of HMM with cross-linked heads determined by electron microscopy was equal to that of the cross-linked NH_2-terminal 24K tryptic fragments of HMM heavy chains determined by NaDodSO$_4$ gel electrophoresis, indicating that this cross-linking is primarily responsible for the contact observed between two HMM heads. Most pairs of the contacted heads originated in the same HMM molecule, although a few pairs belonged to different HMM molecules. Cross-linking between the two heads of the same HMM molecule appeared to occur within the distal, more globular half of each head. However, the cross-linking sites were located at different positions within the globular portion. The actin-activated Mg-ATPase activity of the HMM sample treated with EDC in the presence of actin increased in a biphasic manner, depending on the concentration of F-actin, with two apparent association constants: 2.9×10^4 M^{-1} and one much less than 1×10^4 M^{-1}. Since the apparent association constant obtained with the HMM control was similar to the latter value, the association constant for HMM molecules with cross-linked heads was identified to be the former value. The binding of HMM to actin was thus strengthened at least by a factor of 3 by the cross-linking between two HMM heads. These results suggest that HMM heads are trapped by treatment with EDC in the rigor complex configuration and that this configuration is retained even after the HMM has been released from actin. The EDC reactivity of rabbit skeletal muscle HMM, however, was different from that of chicken gizzard HMM. The treatment of acto–HMM complexes with EDC did not generate cross-linking between two skeletal muscle HMM heads.

Actin and myosin are two essential proteins for muscular contraction. The myosin molecule contains two pear-shaped heads at one end of a long tail (Slayter & Lowey, 1967). The heads are important, because they bear the actin binding capability, the ATPase activity (Mueller & Perry, 1962), and the site for binding of regulatory light chains (Szent-Györgyi et al., 1973). Moreover, because of their cyclic interaction with actin, they are believed to be involved in the generation of the contractile force (Huxley, 1969). Our recent carbodiimide cross-linking study with the rigor acto–smooth muscle

† This work was supported by Grant-in-Aids for Special Project Research, "Calcium Ions and Cell Function" and "Metabolic Researches of Blood Vessels", from the Ministry of Education, Science and Culture of Japan and by Research Grants for Cardiovascular Diseases (60C-1 and 62A-3) from the Ministry of Health and Welfare.

* Address correspondence to this author.

0006-2960/90/0429-3013$02.50/0

heavy meromyosin (HMM)[1] complex has demonstrated that the two heads of a HMM molecule are in contact with each other (Onishi et al., 1989a). It was the first clear demonstration of the actin-dependent interaction between two myosin heads. Since the reason why a myosin molecule has two heads is still unknown, this finding may provide a clue to the puzzle. Nevertheless, the nature and location of the head-to-head interaction are poorly understood.

The structural features of the actin–myosin head interaction region have been extensively investigated with isolated rabbit skeletal muscle myosin heads (myosin subfragment 1). The three-dimensional structure of actin filaments decorated with subfragment 1 was reconstructed from their electron microscopic images (Moore et al., 1970; Taylor & Amos, 1981; Toyoshima & Wakabayashi, 1985). These results indicated that actin binding occurred in the distal half of the head region. Chemical cross-linking experiments of acto–subfragment 1 complexes showed that two tryptic heavy-chain fragments of approximate molecular weights 20K and 50K cross-linked to actin (Mornet et al., 1981). More precise mapping studies of the cross-linking sites on the heavy-chain sequence have been performed by using a chemical cleavage technique (Sutoh, 1982, 1983). The results of these studies indicate that an actin-binding site is near the junction of 50K/20K fragments. On the basis of these electron microscopic and chemical studies, we now have a common understanding about the actin-binding region of myosin. In contrast, the head-to-head cross-linking has just recently been demonstrated. Only the gross primary structure has been investigated so far by cyanogen bromide cleavage followed by HPLC mapping (Onishi et al., 1989b). Two cross-linking sites were located in the NH_2-terminal 24K region of the HMM heavy chain. Their location in the amino acid sequence was far from that of the actin-binding sites.

In the present paper, the spatial location of the cross-linking sites was visualized by electron microscopy of EDC-treated HMM molecules. The result indicates that both of the sites are located in the distal half of HMM heads. The HMM sample with cross-linked heads also provides a valuable tool for investigating the function of the head-to-head interaction. The result shows that the binding affinity of HMM with actin during the ATPase reaction was strengthened by the covalent cross-link between two HMM heads.

Materials and Methods

Preparations of Proteins. Myosin was prepared from chicken gizzard by our routine method (Ikebe et al., 1978). Chicken gizzard HMM was obtained by digestion of myosin with trypsin (Onishi et al., 1989a) and purified by chromatography on a DEAE-cellulose column. Figure 1 shows an elution profile. Fractions contained within the front two-thirds of the second protein peak were pooled. HMM could be separated from subfragment 1 (the first peak) by this chromatographic procedure.

Myosin from rabbit skeletal muscle was prepared according to the method of Perry (1955). Rabbit skeletal muscle HMM was obtained by tryptic digestion of myosin essentially according to the method of Weeds and Taylor (1975), described for α-chymotryptic digestion. Actin was isolated from rabbit skeletal muscle by the method of Spudich and Watt (1971).

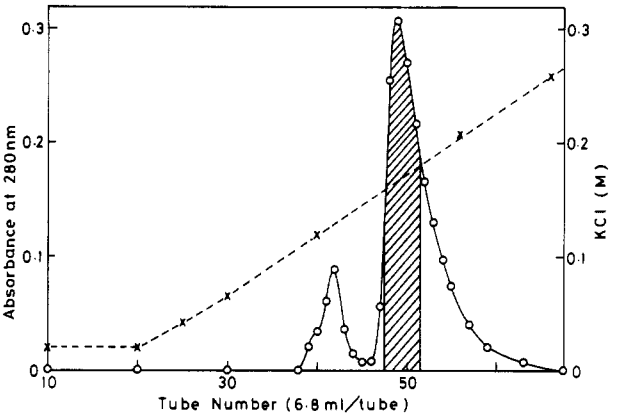

FIGURE 1: Elution profile of a DEAE-cellulose column used to isolate HMM from a tryptic digest of gizzard myosin. The myosin digest (200 mg) was dialyzed overnight against 20 mM KCl, 20 mM Tris-HCl (pH 7.5), 10 mM $MgCl_2$, and 0.3 mM DTT. The insoluble aggregates thus produced were removed by ultracentrifugation at 100000*g* for 1 h. The clear supernatant was then applied to a 2.1 × 23 cm column of DEAE-cellulose equilibrated with 20 mM KCl, 2 mM $MgCl_2$, 20 mM Tris-HCl (pH 7.5), 0.1 mM EDTA, and 0.3 mM DTT. The bound proteins were eluted with a 600-mL linear gradient (20–500 mM) of KCl at a flow rate of 26.5 mL/h. The hatched area in the second protein peak was collected and used as pure HMM.

Fluorescent Labeling of Proteins. Labeling of rabbit skeletal muscle HMM was carried out with a fluorescent dye, *N*-(iodoacetyl)-*N'*-(5-sulfo-1-naphthyl)ethylenediamine (IAEDANS), as reported by Takashi et al. (1976). Under these conditions, the reactive thiol group of HMM, SH_1, was selectively modified by AEDANS. F-Actin was labeled with a fluorescent dye, *N*-[7-(dimethylamino)-4-methyl-3-coumarinyl]maleimide (DACM), under the conditions specified in a previous paper (Onishi et al., 1989a).

EDC Treatment of Acto–HMM Complex and Isolation of Head-to-Head Cross-Linked HMM from the EDC Reaction Mixture. Gizzard HMM (0.5 mg/mL) in 0.1 M KCl, 10 mM $MgCl_2$, and 10 mM imidazole hydrochloride (pH 7.0) was mixed with rabbit skeletal muscle F-actin at a molar ratio of actin/HMM head = 1. The cross-linking reaction was performed by incubating the acto–HMM complex with freshly prepared 5 mM EDC for 1 h at 24 °C. The reaction was terminated by adding 30 mM 2-mercaptoethanol. The details of the procedure were described in a previous paper (Onishi et al., 1989a). After the reaction, the mixture was dialyzed overnight against 0.1 M KCl, 2 mM $MgCl_2$, 0.3 mM DTT, and 10 mM Tris-HCl (pH 7.5), adjusted to 1.5 mM ATP, and then centrifuged at 150000*g* for 90 min to remove actin and HMM irreversibly linked with actin in a pellet. The supernatant was centrifuged again under the same conditions but in the absence of ATP to remove a trace amount of remaining actin. The supernatant containing HMM with cross-linked heads was collected. EDC treatment of the rabbit skeletal muscle acto–HMM complex was carried out similarly.

Determination of HMM Concentrations in Isolated Head-to-Head Cross-Linked HMM Preparation and Cross-Linked Acto–HMM Complex. As described above, the EDC-treated acto–HMM was separated into a supernatant and a pellet by ultracentrifugal fractionation. The protein concentration of the supernatant was determined with the BCA protein assay (Smith et al., 1985). However, the amount of HMM in the pellet could not be determined by the same assay, because the pellet also contained actin. The pellet was thus subjected to $NaDodSO_4$ gel electrophoresis. The amount of

[1] Abbreviations: HMM, heavy meromyosin; ALC_1 and ALC_2, alkali light chains 1 and 2 of skeletal muscle myosin; ATPase, adenosine-5'-triphosphatase; EDC, 1-ethyl-3-[3-(dimethylamino)propyl]carbodiimide; IAEDANS, *N*-(iodoacetyl)-*N'*-(5-sulfo-1-naphthyl)ethylenediamine; DACM, *N*-[7-(dimethylamino)-4-methyl-3-coumarinyl]maleimide; DTT, dithiothreitol; Tris-HCl, tris(hydroxymethyl)aminomethane hydrochloride; $NaDodSO_4$, sodium dodecyl sulfate.

HMM was estimated by densitometric scanning of the Coomassie blue stained gel. The amount of actin was obtained by subtracting the amount of HMM from the total amount of protein.

$NaDodSO_4$ Gel Electrophoresis. Gel electrophoresis was carried out according to Laemmli (1970), using slab gels containing 11% acrylamide and 0.3% bis(acrylamide). Gels were stained with Coomassie brilliant blue. Fluorescent bands were observed under a long-wavelength ultraviolet lamp before the gel was stained. The Coomassie blue stained gels were scanned at 633 nm with a laser scanning densitometer (LKB ultrascan XL). The relative amounts of the 24K and 68K heavy-chain fragments of gizzard HMM and their EDC-catalyzed cross-linked dimers were estimated from the peak area of each band determined by densitometric scanning of the gel.

Electron Microscopy. HMM samples (about 1 mg/mL) were dialyzed overnight at 4 °C against 1 M ammonium acetate containing 0.3 mM DTT to remove nonvolatile salts. The samples were diluted to 10 μg of myosin/mL in 60% glycerol and 1 M ammonium acetate immediately before being sprayed. They were sprayed onto freshly cleaved mica as described by Tyler and Branton (1980). The mica sheets were mounted on the rotary stage in a freeze-etching apparatus (JFD-9000, JEOL) and dried in vacuo at room temperature. HMM molecules on mica were shadowed by platinum/carbon at an angle of 8° from an electron gun while the stage was rotated. Platinum replicas were carbon-coated and examined in a JEOL 2000FX electron microscope at an accelerating voltage of 120 kV. The magnification was calibrated by using a carbon replica of 2140/mm grating purchased from Nissin EM Co., Tokyo, Japan.

ATPase Activities. The Mg-dependent and actin-activated Mg-dependent ATPase activities were measured at 37 °C in a solution containing 50 mM KCl, 2 mM $MgCl_2$, 0.3 mM DTT, 20 mM Tris-HCl (pH 7.5), and 1 mM ATP unless otherwise noted. For assays in the presence of actin, various amounts of F-actin (0–4 mg) were added to 1 mL of the reaction medium. The ATPase reaction was stopped by addition of 7% trichloroacetic acid. Inorganic phosphate was determined colorimetrically according to the method of Youngburg and Youngburg (1930) using stannous chloride.

Results

Isolation of Gizzard HMM with Cross-Linked Heads. Gizzard HMM in the presence and absence of actin was cross-linked by the EDC-catalyzed reaction specified under Materials and Methods. Figure 2 shows $NaDodSO_4$ gel electrophoretic patterns of various EDC cross-linked products. The heavy chain of the tryptically digested gizzard HMM we used consisted of three fragments of approximate molecular weights 24K, 50K, and 68K (lane A). As shown in lane B of this figure, only one new species of approximate molecular weight 110K was produced during EDC treatment of gizzard HMM in the absence of actin. The 110K band became fluorescent when a cross-linking experiment was carried out with HMM whose 68K heavy-chain fragment had been labeled with fluorescent AEDANS (data not shown). Since two HMM heavy chains are noncovalently associated with each other at their subfragment 2 regions, we conclude that the 110K species is a cross-linked product of two 68K fragments (probably via their subfragment 2 regions) which contain the COOH-terminal region of the HMM heavy chain (Figure 3, double arrow). The peak area of the 110K band in lane B was quantitated by gel densitometry and was about 11% of the sum of the peak areas of the 68K and 110K bands. This result

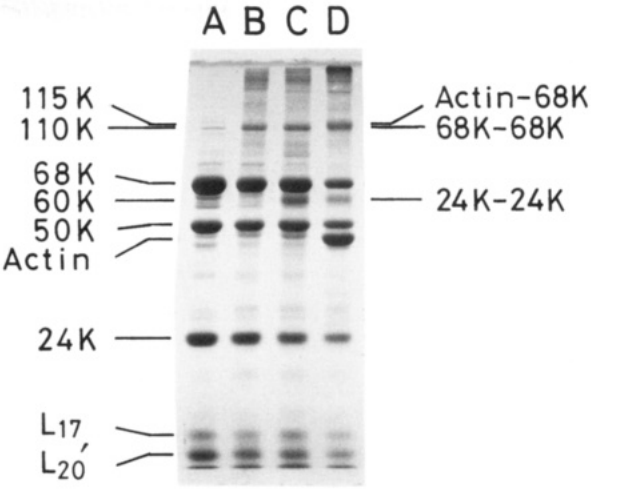

FIGURE 2: $NaDodSO_4$ gel electrophoretic patterns of various EDC cross-linked samples of gizzard HMM. (A) Untreated gizzard HMM. (B) Gizzard HMM treated with EDC in the absence of actin. (C) Supernatant obtained from the EDC reaction mixture of acto–gizzard HMM by ultracentrifugation in the presence of Mg-ATP. (D) Pellet obtained from the same reaction mixture as in (C). The gel was stained with Coomassie brilliant blue. The bands identified as 24K, 50K, and 68K represent tryptic fragments of the HMM heavy chain. L_{17} and L_{20}' indicate the 17K light chain of HMM and the tryptic fragment of the HMM 20K light chain, respectively. The positions of the three cross-linked products found in acto–gizzard HMM are identified on the right margin of the gel: 24K–24K (60K), 68K–68K (110K), and actin–68K (115K). The 60K band is present in (C) and (D) but not in (A) and (B). The 115K band is observed only in (D). The 110K band is observed in (B) and (C). Whether or not the 110K band is present in (D) is unclear, because this band overlaps with the 115K band. A faint band was observed around 110K in (A), but it is not a cross-linked product. Note that EDC treatment produced many high molecular weight bands (B, C, and D).

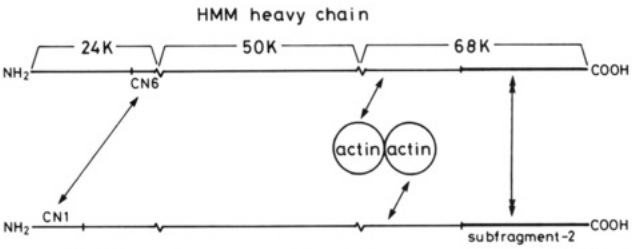

FIGURE 3: Schematic representation of the two covalently cross-linked sites by carbodiimide between two HMM heavy chains (long arrow and double arrow) and covalently cross-linked sites between actin and HMM heavy chains (short arrows). Three heavy-chain fragments (24K, 50K, and 68K) are generated by tryptic digestion of HMM. Two heavy chains of an HMM molecule are associated with each other at their COOH-terminal regions (subfragment 2) to form the tail portion of HMM. CN1 and CN6 are fragments containing Ser1–Met77 and Leu164–Lys203, respectively, produced by cyanogen bromide cleavage of the NH_2-terminal 24K segment of the HMM heavy chain.

suggests that about 11% of the 68K fragments are dimerized by the cross-linking. We used this product as an EDC-treated HMM control for various experiments, because the same cross-link between two 68K fragments must occur also in the case of EDC treatment under the same conditions but in the presence of actin.

After gizzard HMM was cross-linked in the presence of actin, the mixture was separated into a supernatant and a pellet by ultracentrifugation in the presence of Mg-ATP as described under Materials and Methods. The gel pattern of the pellet (lane D in Figure 2) shows two new bands with approximate molecular weights of 60K and 115K as major cross-linked products. These species have been previously reported to be

Table I: Occurrence of Different Types of Head-to-Head Contacts Observed in Chicken Gizzard HMM Preparations Treated with EDC in the Presence or Absence of Actin

	no contact[a] (A)	intramolecular contact[b] (B)	intermolecular contact[c] (C)	total double-headed HMM (A + B + 2C)	total single-headed HMM	proportion of head-to-head contact[d]
untreated HMM	1619	44	0	1663	42	2.6
HMM treated with EDC in the absence of actin	1532	161	0	1693	47	9.5
HMM treated with EDC in the presence of actin	1071	786	5	1867	61	42.4

[a] The two heads of an HMM molecule are not in contact with each other. [b] The two heads of an HMM molecule are in contact with each other. [c] The two heads, each belonging to different HMM molecules, are in contact with each other. [d] $[(B + C)/(A + B + 2C)] \times 100$.

covalently linked complexes between two 24K heavy-chain fragments originating from the NH_2-terminal portion of HMM heavy chains and between actin and the COOH-terminal 68K heavy-chain fragment, respectively (Onishi et al., 1989a; also see Figure 3). Actin and actin-containing 115K bands were observed in the pellet (lane D), but not in the supernatant (lane C), indicating that the HMM irreversibly cross-linked with actin also cosedimented with the actin during ultracentrifugation.

In contrast to the actin-containing bands, two cross-linked complexes with approximate molecular weights of 60K and 110K remained dissolved in the supernatant even after ultracentrifugation, as shown in lane C of Figure 2. The peak area of the 60K band was estimated to be 34% of the sum of the peak areas of the 24K and 60K bands as determined by gel densitometry. Since the 60K band is the cross-linked product of two 24K fragments as already described, it appears that 34% of the pairs of HMM heads cross-link to each other via their NH_2-terminal heavy-chain regions. Therefore, the cross-linking reaction produced a mixture of HMM with either bound or unbound heads. The 110K band was the same in its electrophoretic mobility and peak area as the 110K band produced by EDC treatment of gizzard HMM in the absence of actin (see lane B). We thus conclude that this product is also a dimer of the 68K fragments and that cross-linking between two 68K regions does not require the presence of actin.

Electron Microscopy of Head-to-Head Cross-Linked HMM. HMM molecules contained in the supernatant (see lane C in Figure 2) were examined by electron microscopy after rotary shadowing with platinum/carbon. Rotary-shadowed images showed that about half of the HMM molecules had a contact between two heads (Figure 4). Most of the contacts were observed between two heads of the same molecule (rows e–h). Contact was also observed between two heads from different molecules, although this was rare (row i). The remaining molecules showed no contact between heads of the same molecule or of different molecules (rows a–d).

Table I shows a summary of the morphological data. A total of 1867 double-headed HMM molecules that had been treated with EDC in the presence of actin were classified according to the criteria described in Table I. We found that 786 molecules had head-to-head contact in the same molecule and only 5 molecules had contact between two heads of different molecules. Therefore, the percentage of head-to-head contact was calculated to be 42.4% of the total molecules. Practically no head-to-head contact occurred when gizzard HMM was sprayed onto mica without cross-linking (Figure 5A and also see Table I). The HMM treated with EDC in the absence of actin also showed head-to-head contact (Figure 5B, row h, images 8–12). However, the percentage of head-to-head contact was only 9.5% of all the molecules scored (Table I). Since the chemical linkage between two 24K heavy-chain fragments was induced by the EDC cross-linking reaction in the presence, but not in the absence, of actin, the difference between 42.4% and 9.5% may be attributed to the cross-linking between two 24K fragments. In fact, this difference (32.9%) was very close to the densitometrically estimated amount (approximately 34%) of the 60K band formed by the cross-linking reaction between two 24K fragments.

Our analysis of the images of the contacted heads (rows e–h of Figure 4) indicated that the two HMM heads were in contact laterally. The distal halves of the heads appear more globular and are connected to a tail via the narrow neck regions. Since a large crevice was frequently observed in the neck region of the contacted heads, it seems unlikely that cross-linking sites belong to the neck region. Therefore, we conclude that two cross-linking sites are located in the distal half of HMM heads.

Noncontacted heads appeared to be flexibly attached to the tail, such that these heads showed a wide range of angles with respect to the tail as illustrated in rows a–d of Figure 4. However, the rotary-shadowed molecular images of two heads cross-linked with EDC (rows e–h) indicated that cross-linking caused some constraint in the molecular morphology. The overall appearance resembled the shape of a tobacco pipe and the molecules look as if they were trapped in this configuration. Since the two heads were cross-linked while they were bound to actin in rigor, it is likely that the rigor configuration of the EDC-treated heads is maintained even after they are released from actin. Therefore, we propose that the two heads of HMM complexed with actin have essentially the same shape as the contacted heads seen in rows e–h.

The two heads of a single HMM molecule appear similarly shaped if they are not contacted (Figure 4, rows a–d). However, we often got the impression that the shapes of the two connected heads were different; while one head looked roundish, the other head looked rather elongated. Moreover, the distal edge of the elongated head was often further protruded than the roundish head (see, for example, Figure 4, row f, images 5, 6, 7, and 10, and row g, images 5, 8 and 11). These morphological features were not limited to the molecules shaped like a tobacco pipe. Some HMM molecules had their connected heads more parallel than perpendicular to the tail (Figure 4, row e, images 1–3), and some heads were folded back on the tail (Figure 4, row h, images 10–12). Since the dissimilar appearance of the two connected heads of a single HMM molecule does not depend upon any special orientation, it is unlikely that the difference is artifactually made. We suggest that the dissimilar morphology is caused by the cross-linking of the two heads and that the cross-linking sites are located at two different areas within each head. This latter interpretation is consistent with our previous biochemical data (Onishi et al., 1989b).

The distribution of the length of the HMM tail is shown in Figure 6. One small peak at 38 nm and two large peaks around 50 nm were observed, indicating that three different

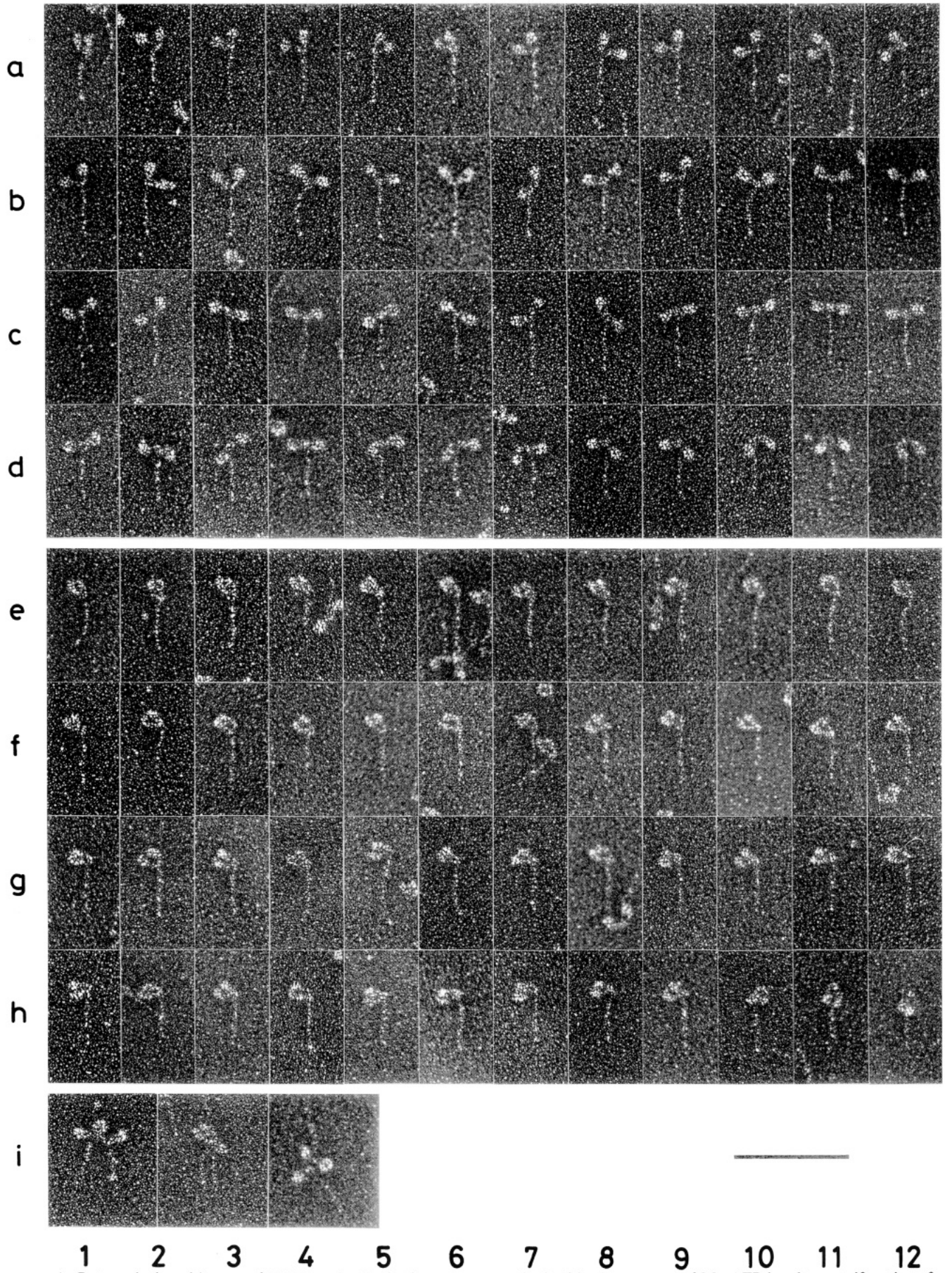

FIGURE 4: Rotary-shadowed images of HMM molecules in the supernatant obtained in the presence of Mg-ATP by ultracentrifugation of acto–gizzard HMM treated with EDC. In rows a–d, the two heads of an HMM molecule are separated from each other. In rows e–h, the two heads in the same HMM molecule are in contact with each other. In row i, the two heads belonging to different HMM molecules are in contact with each other. The molecules are arranged so that the first molecules appearing in each series have their heads extended upward while those appearing toward the end of each series have their heads draped over the tail. Magnification: 217000×. The scale bar represents 100 nm.

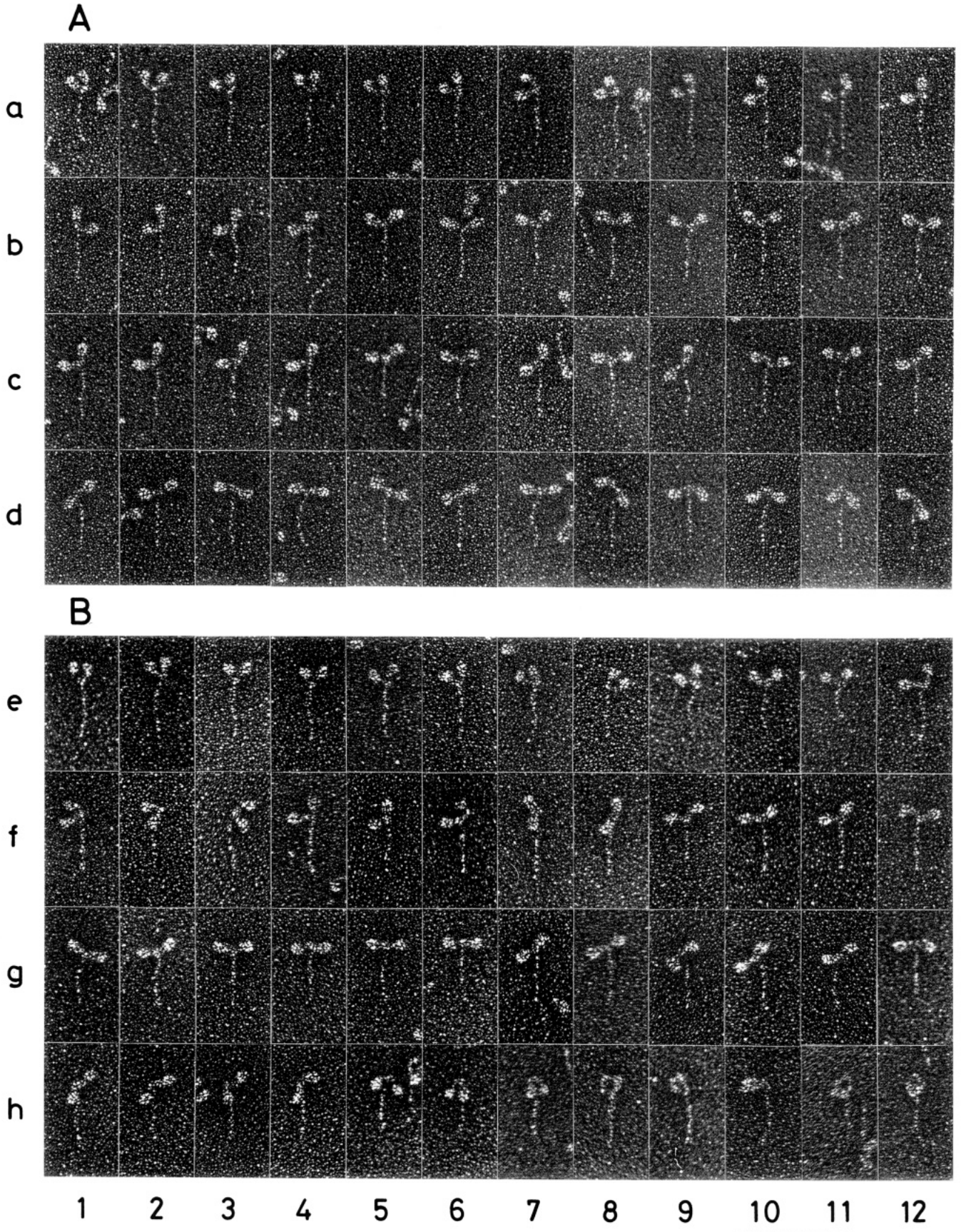

FIGURE 5: Rotary-shadowed images of untreated HMM molecules (A) and those treated with EDC in the absence of actin as a control (B). In images 8–12 of row h, the two heads in the same HMM molecule are in contact with each other. Magnification: 217000×. The scale bar represents 100 nm.

cleavable sites for trypsin are localized in the tail region of gizzard myosin. When the 10S (folded) form of gizzard myosin was investigated by electron microscopy (Onishi & Wakabayashi, 1982), two hinge regions were identified in the tail portion and one of them was located approximately 50 nm away from the head–tail junction. Our present observation

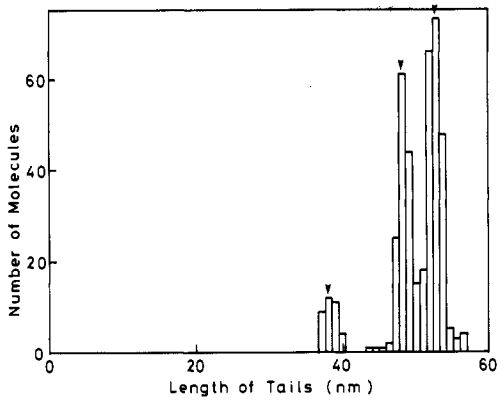

FIGURE 6: Distribution of HMM tail length. Measurements were made from the head–tail junction to the end of the enzymatically cleaved tail. Arrowheads (at 38, 49, and 53 nm) indicate major peaks of the distribution.

suggests that this hinge region is the site on gizzard myosin attacked by trypsin to form HMM.

Effect of Head-to-Head Cross-Linking on the Mg-ATPase and Actin-Activated Mg-ATPase Activities of Gizzard HMM. We reported earlier that the Mg-ATPase activity of acto–gizzard HMM was significantly enhanced by the EDC-catalyzed cross-linking reaction (Onishi et al., 1989a). Earlier, Marianne-Pépin et al. (1985) also reported that the EDC cross-linking of gizzard subfragment 1 to actin stimulated the Mg-ATPase activity of acto–subfragment 1. We interpreted our result to mean that the stimulating effect observed with the cross-linked gizzard HMM might be due to the irreversible binding of the HMM heads to actin. The present study examines whether or not the EDC cross-linking between two HMM heads can induce the stimulation of the Mg-ATPase and actin-activated Mg-ATPase activities. For this purpose, we used the partially purified head-to-head cross-linked product of gizzard HMM isolated from the EDC reaction mixture of acto–HMM as already described.

Figure 7 shows the effect of KCl concentrations on the Mg-ATPase activities of untreated gizzard HMM and three cross-linked products. For a wide range of KCl concentrations, the Mg-ATPase activity of the partially purified head-to-head cross-linked HMM (open squares) was 1.5 times higher than that of untreated HMM (open circles). However, the HMM control obtained by EDC treatment under the same conditions but in the absence of actin (open triangles) also showed increased activities. This latter result indicates that the HMM Mg-ATPase activity itself is not substantially affected by the production of the covalent bridge between two 24K heavy-chain fragments of HMM. The Mg-ATPase activity of the covalently linked acto–HMM complex sedimented as the pellet is also shown in Figure 7 (closed squares). This activity was 6 times higher than the activity measured with the partially purified head-to-head cross-linked HMM. This result is consistent with our previous proposal that the enhanced Mg-ATPase activity of the EDC-treated acto-gizzard HMM is due to the irreversible binding of the HMM heads to actin (Onishi et al., 1989a).

Various concentrations of F-actin were added to untreated gizzard HMM and two EDC-treated products, and their Mg-ATPase activities were measured (Figure 8). The Mg-ATPase activity of the partially purified head-to-head cross-linked HMM (open squares) rapidly increased until the actin concentration reached about 40 μM. Beyond this concentration, the slope of the activity increase gradually slowed down to the level observed with untreated gizzard HMM (open circles). This result suggests that there are two association

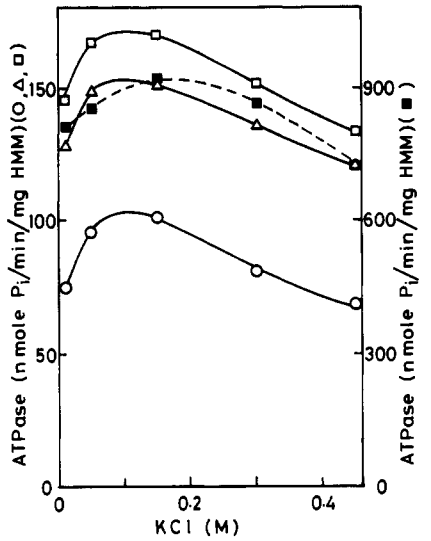

FIGURE 7: Mg-ATPase activities of various HMM samples as a function of KCl concentration. Untreated gizzard HMM (○), the sample obtained by EDC treatment of gizzard HMM in the absence of actin (△), and the supernatant (□) and pellet (■) obtained by ultracentrifugation in the presence of Mg-ATP of the EDC reaction mixture of acto–gizzard HMM were submitted to Mg-ATPase assay at 37 °C in 2 mM $MgCl_2$, 20 mM Tris-HCl (pH 7.5), 0.3 mM DTT, and 1 mM ATP. The HMM concentration of each sample was 0.04 mg/mL except for the pellet, in which the concentrations of HMM and actin components in the cross-linked acto–HMM complex were 0.018 and 0.015 mg/mL, respectively.

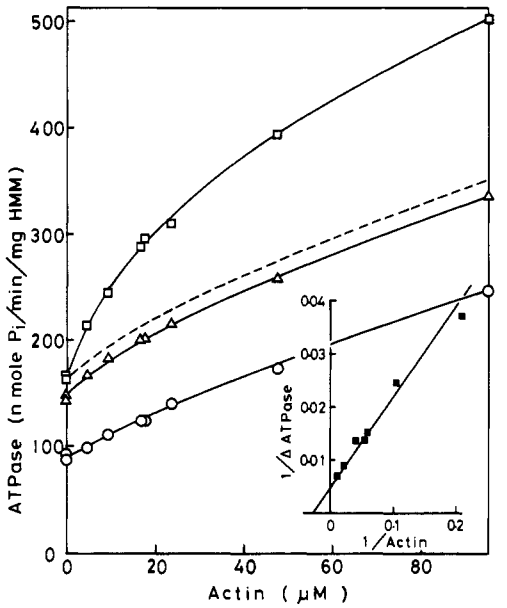

FIGURE 8: Actin-activated Mg-ATPase activities of various HMM samples as a function of F-actin concentration. Symbols for HMM samples (○, △, □) are the same as described in Figure 7. The concentration of HMM was 0.04 mg/mL and the actin concentration was varied between 0 and 4 mg/mL. The ATPase assay was carried out at 37 °C in 50 mM KCl, 2 mM $MgCl_2$, 20 mM Tris-HCl (pH 7.5), 0.3 mM DTT, and 1 mM ATP. The broken line, which indicates the base-line level of activity, is the parallel shift of the line formed by HMM treated with EDC in the absence of actin (△). Note that the shifted amount is the difference in activities measured with no actin. The inset shows a double-reciprocal plot of the actin-activated Mg-ATPase activity of the head-to-head cross-linked HMM remaining in the supernatant as a function of the actin concentration. The values for the ATPase activity (Δ ATPase) used for this plot are the differences between the activity of the supernatant (□) and the broken line. From the intercept of the line with the abscissa, the association constant was determined to be 2.9×10^4 M^{-1}.

constants for the partially purified head-to-head cross-linked HMM. The slope of the monophasic increase seen with the

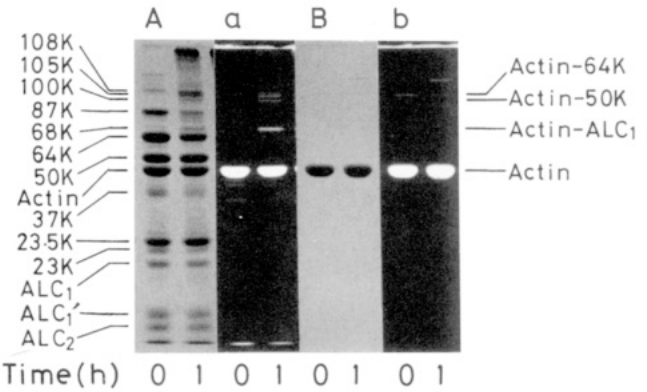

FIGURE 9: Carbodiimide-catalyzed cross-linking of the rigor complex formed between DACM-modified actin and rabbit skeletal muscle HMM. Tryptically digested skeletal muscle HMM (1.0 mg/mL) was mixed with DACM-modified F-actin at a molar ratio of actin/HMM head = 1. The cross-linking reaction was carried out as specified under Materials and Methods for 0 (not cross-linked) and 1 h as indicated at the bottom of each lane. Protein samples (10 μg of HMM) were submitted to gel electrophoresis in the presence of $NaDodSO_4$. Coomassie blue stained gels (A and B) and their fluorographs (a and b) are shown as pairs. The bands indicated as 23K, 23.5K, 37K, 50K, 64K, and 87K are the tryptic fragments of the HMM heavy chain. Among these fragments, 23.5K, 50K, and 64K are the major ones. ALC_1 and ALC_2 are the alkali light chains 1 and 2 of HMM, respectively, and ALC_1' is the tryptic fragment of ALC_1. The bands indicated as 68K, 100K, 105K, and 108K are four cross-linked species. The 68K, 100K, and 105K bands are fluorescent, whereas the 108K band is not. As a control, fluorescent F-actin was treated with EDC (B). The 68K, 100K, 105K, and 108K bands are not seen by Coomassie blue staining (B) nor in the fluorograph (b). The higher M_r bands of approximately 110K and 160K (a) are not products of the actin–HMM cross-linking reaction, as they are formed when actin alone is treated with EDC (b). The positions of the three cross-linked products found in acto-skeletal muscle HMM are identified on the right margin of the gel: actin–ALC_1 (68K), actin–50K (100K), and actin–64K (105K).

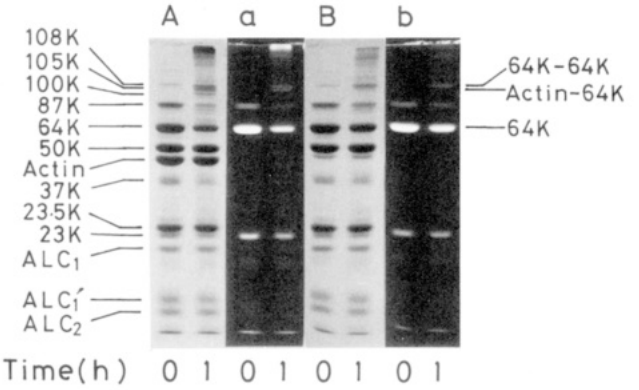

FIGURE 10: Identification of the rabbit skeletal muscle HMM components that participate in the EDC-catalyzed cross-linking reaction. The fluorescent labeling was carried out by incubating skeletal muscle HMM with IAEDANS as specified under Materials and Methods. Conditions for the cross-linking reaction with EDC and for $NaDodSO_4$ gel electrophoresis were the same as described in Figure 9. Coomassie blue stained gels (A and B) and their fluorographs (a and b) are shown as pairs. The COOH-terminal 64K fragment of the HMM heavy chain is strongly labeled with fluorescent AEDANS. The 87K and 23K bands are also fluorescent, but they appear to be precursor and breakdown materials, respectively, of the 64K fragment. The 100K, 105K, and 108K bands are cross-linked products (A). The 105K and 108K bands are fluorescent, whereas the 100K band is not. EDC treatment of AEDANS-modified skeletal muscle HMM in the absence of actin was performed as a control. Only one band (108K) is observed both by Coomassie blue staining (B) and by fluorescence (b). No cross-linked product between two HMM heads is detected.

Mg-ATPase activity of the EDC-treated HMM control (open triangles) was also similar to that obtained with untreated gizzard HMM. The binding of actin to the EDC-treated HMM control was too weak to determine the exact association constant. However, it was roughly estimated to be much less than 1×10^4 M^{-1}.

The double-reciprocal plot of the actin-activated Mg-ATPase activity of the partially purified head-to-head cross-linked HMM versus the actin concentration is shown in the inset of Figure 8. The activity values used to make this plot were the difference between the measured values (open squares) and the estimated basal activity values shown in Figure 8 by the broken line. This correction should isolate the activity increase induced by the HMM with cross-linked heads. From this plot, the association constant and the maximum activity were determined to be 2.9×10^4 M^{-1} and 200 nmol min^{-1} (mg of HMM)$^{-1}$, respectively. Analysis by $NaDodSO_4$ gel electrophoresis of the partially purified head-to-head cross-linked sample used in this enzymatic activity assay revealed that the population of the HMM molecules with cross-linking between two 24K heavy-chain fragments was only 26% of the total HMM and the remaining HMM did not have such cross-linking. Taking this result into consideration, we conclude that the heterogeneity of the HMM sample is responsible for the presence of two apparent association constants.

Does Head-to-Head Cross-Linking Occur within the Skeletal Muscle Acto–HMM Complex? A cross-linking study on the rabbit skeletal muscle HMM in the presence of fluorescently labeled actin was performed by using the EDC-catalyzed reaction. The $NaDodSO_4$ gel electrophoretic patterns from the experiment are shown in panel A of Figure 9. The gel pattern at time 0 shows that the skeletal muscle HMM preparation we used consisted of five major components: three heavy-chain fragments having molecular weights of 23.5K, 50K, and 64K and two alkali light chains, ALC_1 and ALC_2. Four new polypeptide species, having approximate molecular weights of 68K, 100K, 105K, and 108K, are produced by the 1-h cross-linking reaction. On the basis of their electrophoretic mobilities, the newly formed 68K and 100K bands were determined to be the cross-linked products between actin and ALC_1 and between actin and the 50K HMM heavy-chain fragment, respectively, because other investigators had already identified those products in their EDC cross-linking studies of rabbit skeletal muscle acto–subfragment 1 (Mornet et al., 1981; Sutoh, 1983). The photograph of the same gel slab under ultraviolet light is illustrated in panel a of Figure 9. It shows that the 68K, 100K, and 105K species are fluorescent, indicating that they contain actin. These products did not appear after actin alone was treated with EDC (panels B and b).

In order to determine how the 108K cross-linked product was generated, cross-linking experiments were also carried out with rabbit skeletal muscle HMM labeled with fluorescent AEDANS (Figure 10). The 64K band was strongly fluorescent although the 87K and 23K bands were also labeled (panel a, time 0; for details, see figure legend). By comparing the protein band patterns shown in the two lanes in panel A, we identified 100K, 105K, and 108K bands as EDC cross-linked products. It is interesting to note that the 68K band was not detected. The site on ALC_1 that could cross-link to actin to form 68K may be masked by the chemical modification by IAEDANS at the reactive thiol SH_1 on HMM heavy chains. Among the three bands, the 105K and 108K bands were fluorescent (panel a, time 1 h), thus suggesting that these species contain the 64K fragment as a component. Since the 105K band was also fluorescent when fluorescent actin was used, this species was identified as a cross-linked product between actin and the 64K fragment of the HMM heavy

chain. On the other hand, the 108K species did not contain actin. Since this species was also produced after EDC treatment of HMM in the absence of actin (panels B and b) and since two HMM heavy chains interact with each other at their subfragment 2 regions where the 64K fragment is located, the 108K band seems likely to be the dimer of the 64K fragment cross-linked intramolecularly at the subfragment 2 region. These analyses show that the EDC treatment does not generate cross-linking between two skeletal HMM heads. This result is contrary to the result obtained with gizzard HMM.

Discussion

In our previous studies (Onishi et al., 1989a,b), we demonstrated that EDC cross-linking of the rigor gizzard acto–HMM complex produced HMM cross-linked with actin as well as HMM with cross-linked heads. The head-to-head cross-linked HMM could be reversibly released from actin in the presence of Mg-ATP, if it was not covalently linked with actin. In the present study, we showed that approximately one-third of the total HMM treated with EDC in the presence of actin could be isolated as HMM with cross-linked heads by ultracentrifugal fractionation in the presence of Mg-ATP. Such HMM preparations could be used to investigate the structure and functional significance of the two HMM heads trapped in the position of rigor.

The most common rotary-shadowed image of head-to-head contacted HMM molecules had the shape of a tobacco pipe (see Figure 4, rows e–h). Since noncontacted HMM heads exhibited no preferred orientation with respect to the tail portion, the asymmetrical appearance of the contacted heads may be caused by the cross-linking of the two heads. If the cross-linking site on each head is the same for both heads, the distances between the connecting site and the tips of the two heads must be equal. However, we noted that the tip of one head was usually further away from the other from the junction between the head and the tail. This observation suggests that the cross-linker joins two HMM heads together at their nonequivalent sites. Consistent with this interpretation is the result of our chemical cleavage study, in which we determined the location of the cross-linking sites on the amino acid sequence of the HMM heavy chain (Onishi et al., 1989b). The result indicated that one cross-linking site resided within the CN1 heavy-chain region on one head of HMM, while the other site belonged to the CN6 heavy-chain region on the other head (see Figure 3). The present electron microscopic study provides visual evidence that supports our earlier proposal.

Both CN1 and CN6 resided within the NH_2-terminal 24K fragment of the HMM heavy chain; the former was the NH_2-terminal peptide of the 24K fragment and the latter was the COOH-terminal peptide of the 24K fragment (Maita et al., 1987). We now show by electron microscopy that the head-to-head cross-linked HMM molecules are connected by the distal, more globular halves of the two heads (see Figure 4). Our observation, then, suggests that the 24K fragment (region) of the HMM heavy chain contributes to the building of the globular portion of HMM heads. The localization of the myosin heavy-chain NH_2-terminal region within the rabbit skeletal muscle myosin head has already been studied by electron microscopy. Three distinct epitopes within the NH_2-terminal 23.5K heavy-chain fragment have been mapped on the myosin head by using monoclonal antibodies (Winkelmann et al., 1983; Winkelmann & Lowey, 1986). These epitopes are all clustered about 14.5 nm from the head–tail junction. In addition, the location of the ATPase site has been determined to be about 14 nm from the head–tail junction, by using a biotinylated ADP analogue on the skeletal muscle myosin head (Sutoh et al., 1986). Furthermore, the NH_2 terminus of the myosin heavy chain has been localized by immunolabeling to about 12 nm from the head–tail junction (Sutoh et al., 1987). All of these electron microscopic studies indicated that the 23.5K fragment sequence was located at the distal half of the myosin head. Although the types of myosins employed are different, the results obtained with the skeletal muscle myosin are consistent with our present observation that the two cross-linking sites, residing within the NH_2-terminal 24K fragments of gizzard HMM heavy chains, are located in the distal half of HMM heads.

When actin filaments that were partially decorated with scallop HMM molecules were examined by electron microscopy, the attached individual HMM molecules could be observed (Craig et al., 1980). This study revealed that the two heads of an HMM molecule were usually attached to neighboring actin monomers on the same helical strand of actin and that the two heads appeared to form approximately the same angle with actin. Since the arrowhead morphology of actin filaments decorated with gizzard HMM was indistinguishable from the arrowhead formed by scallop HMM (Kendrick-Jones et al., 1982), the two heads of gizzard HMM are expected to form the same angle with actin. As illustrated in Figure 11, the two heads must be asymmetrically positioned in order to maintain the same angle between the actin filament and the head axes. Therefore, the asymmetric profile of the contacted HMM heads demonstrated in the present study (rows e–h in Figure 4) may be imposed by the rigor link formation with actin filaments and trapped by the cross-linking reaction.

Figure 11 also illustrates two possible models for the attachment of gizzard HMM heads to actin filaments. As indicated by the curved lines in HMM heads, an NH_2-terminal 24K HMM heavy-chain fragment must span across the globular HMM head. This accommodates contacts between CN1 and CN6. The two models are opposite with respect to the position of CN1 and CN6 regions. When the two heads are attached to neighboring actin monomers, the CN1 region of one head of HMM faces the CN6 region of the other head in both models, so that CN1 and CN6 can be cross-linked with EDC.

In the present study, actin filaments fully decorated with gizzard HMM molecules (the molar ratio of actin/HMM head = 1) were prepared for the EDC cross-linking reaction. Nevertheless, most of the cross-linked heads were in the same HMM molecule, and very few belonged to different HMM molecules. It thus appears that head-to-head contact occurs much more frequently within the same HMM molecule than between two neighboring HMM molecules, although the positional relationship between CN1 and CN6 is the same. This indicates that at rigor the distance between two myosin heads is larger when the two heads belong to two neighboring myosins than when they belong to the same molecule.

Since the Mg-ATPase activity of gizzard HMM in the absence of actin was unaltered by cross-linking two 24K fragments (see Figure 7), it is unlikely that the EDC cross-linking reaction causes chemical modification of the ATPase active site itself. However, a significant difference was found between head-to-head cross-linked HMM and the HMM control in their actin-activated Mg-ATPase activities (Figure 8). The binding constant for the head-to-head HMM was approximately $2.9 \times 10^4\ M^{-1}$, at least 3-fold stronger than the HMM control. This increased enzymatic activity suggests that two cross-linked heads have cooperativity caused by the covalent bridge between them. In addition to the electron microscopic study already presented, this result further suggests

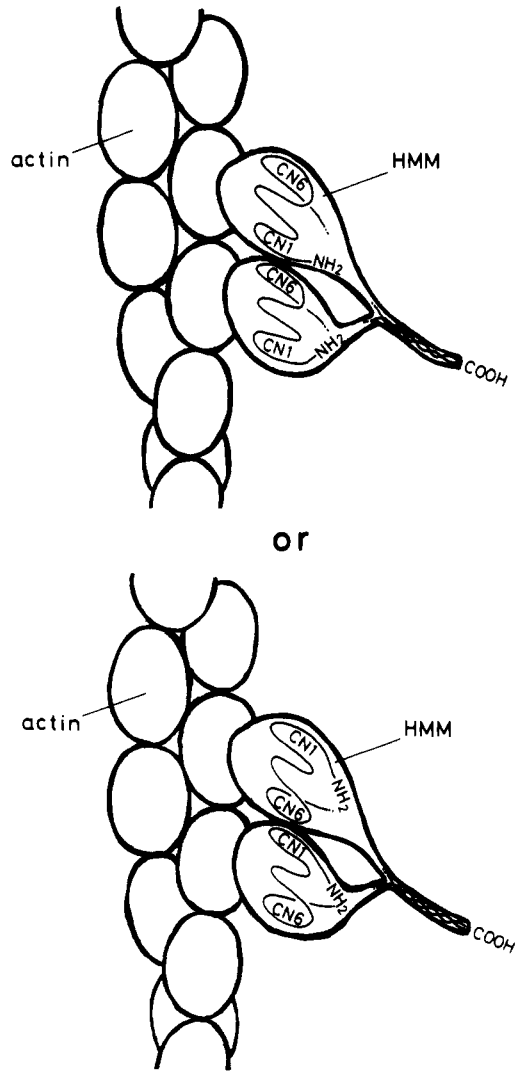

FIGURE 11: Schematic diagram illustrating the relationship of the two heads of gizzard HMM attached to an actin filament in rigor. The two identical HMM heads bind to neighboring actin monomers in the same helical strand. One head is rotated relative to the other by 180°, so that the two heads are oriented in the same direction. The curved line in each head indicates the hypothetically folded NH_2-terminal 24K region of the HMM heavy-chain polypeptide. CN1 and CN6 are peptides produced from the 24K peptide by cyanogen bromide cleavage that span Ser1–Met77 and Leu164–Lys203, respectively. There are two feasible orientations for the two heads. The top diagram shows CN6 facing the top and CN1 the bottom. In the bottom diagram, the reverse case is illustrated. In both cases, the CN1 region of one head of HMM can interact with the CN6 region of the other head.

that the positional relationship between two HMM heads in the rigor complex is trapped by the EDC cross-linking and remains unchanged even after the cross-linked HMM has been released from actin in the presence of Mg-ATP.

Previous kinetic studies (Ikebe et al., 1981; Sellers et al., 1982) indicated that phosphorylation of the 20K light chains of gizzard HMM is accompanied by an approximately 10–25-fold increase in the maximum rate for the actin-activated Mg-ATPase activity and a 3–4-fold increase in the apparent binding constant of HMM to actin. It is interesting to note that this level of increase in the HMM–actin binding constant is similar to the binding constant increase caused by the EDC cross-linking of two HMM heads. Since the 20K light chains are phosphorylated in the contracting smooth muscle, studies on phosphorylated myosin are important. Therefore, EDC cross-linking studies on phosphorylatable gizzard HMM are in progress.

Head-to-head cross-linking could not be detected in the acto–rabbit skeletal muscle HMM complex treated with EDC (see Figures 9 and 10). This is a remarkable difference between skeletal muscle and gizzard HMMs. The homology between skeletal muscle and gizzard myosin heavy-chain sequences was particularly low in the NH_2-terminal CN1 region (Maita et al., 1987), which was shown to be one of the linkage-participating pieces (Onishi et al., 1989b). The lysine or glutamic acid residues required for cross-linking may be replaced by other side chains in skeletal myosin. This is a plausible cause for the lack of EDC-induced cross-linking between two skeletal muscle HMM heads.

In summary, we have demonstrated that HMM treated with EDC in the presence of actin keeps its rigor configuration even after being released from actin. Our previous proposal that the two heads of gizzard myosin interact with each other when cross-bridges are formed (Onishi et al., 1989a,b) becomes more plausible.

ACKNOWLEDGMENTS

We thank Dr. Elena McBeath for her valuable advice throughout the preparation of the manuscript. We also thank Taiko Ohmura for technical assistance.

REFERENCES

Craig, R., Szent-Györgyi, A. G., Beese, L., Flicker, P., Vibert, P., & Cohen, C. (1980) *J. Mol. Biol. 140*, 35–55.

Huxley, H. E. (1969) *Science 164*, 1356–1366.

Ikebe, M., Aiba, T., Onishi, H., & Watanabe, S. (1978) *J. Biochem. (Tokyo) 83*, 1643–1655.

Ikebe, M., Tonomura, Y., Onishi, H., & Watanabe, S. (1981) *J. Biochem. (Tokyo) 90*, 61–77.

Kendrick-Jones, J., Jakes, R., Tooth, P., Craig, R., & Scholey, J. (1982) in *Basic biology of muscles: a comparative approach* (Twarog, B. M., Levine, R. J. C., & Dewey, M. M., Eds.) pp 255–272, Raven Press, New York.

Laemmli, U. K. (1970) *Nature (London) 227*, 680–685.

Maita, T., Onishi, H., Yajima, E., & Matsuda, G. (1987) *J. Biochem. (Tokyo) 102*, 133–145.

Marianne-Pêpin, T., Mornet, D., Bertrand, R., Labbé, J.-P., & Kassab, R. (1985) *Biochemistry 24*, 3024–3029.

Moore, P. B., Huxley, H. E., & DeRosier, D. J. (1970) *J. Mol. Biol. 50*, 279–295.

Mornet, D., Bertrand, R., Pantel, P., Audemard, E., & Kassab, R. (1981) *Nature (London) 292*, 301–306.

Mueller, H., & Perry, S. V. (1962) *Biochem. J. 85*, 431–439.

Onishi, H., & Wakabayashi, T. (1982) *J. Biochem. (Tokyo) 92*, 871–879.

Onishi, H., Maita, T., Matsuda, G., & Fujiwara, K. (1989a) *Biochemistry 28*, 1898–1904.

Onishi, H., Maita, T., Matsuda, G., & Fujiwara, K. (1989b) *Biochemistry 28*, 1905–1912.

Perry, S. V. (1955) in *Methods in Enzymology* (Colowick, S. P., & Kaplan, N. O., Eds.) Vol. 2, pp 582–588, Academic Press, New York.

Sellers, J. R., Eisenberg, E., & Adelstein, R. S. (1982) *J. Biol. Chem. 257*, 13880–13883.

Slayter, H. S., & Lowey, S. (1967) *Proc. Natl. Acad. Sci. U.S.A. 58*, 1611–1618.

Smith, P. K., Krohn, R. I., Hermanson, G. T., Mallia, A. K., Gartner, F. H., Provenzano, M. D., Fujimoto, E. K., Goeke, N. M., Olson, B. J., & Klenk, D. C. (1985) *Anal. Biochem. 150*, 76–85.

Spudich, J. A., & Watt, S. (1971) *J. Biol. Chem. 246*, 4866–4871.

Sutoh, K. (1982) *Biochemistry 21*, 3654-3661.
Sutoh, K. (1983) *Biochemistry 22*, 1579-1585.
Sutoh, K., Yamamoto, K., & Wakabayashi, T. (1986) *Proc. Natl. Acad. Sci. U.S.A. 83*, 212-216.
Sutoh, K., Tokunaga, M., & Wakabayashi, T. (1987) *J. Mol. Biol. 195*, 953-956.
Szent-Györgyi, A. G., Szentkiralyi, E. M., & Kendrick-Jones, J. (1973) *J. Mol. Biol. 74*, 179-203.
Takashi, R., Duke, J., Ue, K., & Morales, M. F. (1976) *Arch. Biochem. Biophys. 175*, 279-283.
Taylor, K. A., & Amos, L. A. (1981) *J. Mol. Biol. 147*, 297-324.
Toyoshima, C., & Wakabayashi, T. (1985) *J. Biochem. (Tokyo) 97*, 219-243.
Tyler, J. M., & Branton, D. (1980) *J. Ultrastruct. Res. 71*, 95-102.
Weeds, A. G., & Taylor, R. S. (1975) *Nature (London) 257*, 54-56.
Winkelmann, D. A., & Lowey, S. (1986) *J. Mol. Biol. 188*, 595-612.
Winkelmann, D. A., Lowey, S., & Press, J. L. (1983) *Cell 34*, 295-306.
Youngburg, G. E., & Youngburg, M. V. (1930) *J. Lab. Clin. Med. 16*, 158-166.

The DNA Binding Domain of GAL4 Forms a Binuclear Metal Ion Complex†

Tao Pan‡ and Joseph E. Coleman*
Department of Molecular Biophysics and Biochemistry, Yale University School of Medicine, New Haven, Connecticut 06510
Received August 4, 1989; Revised Manuscript Received November 27, 1989

ABSTRACT: The transcription factor GAL4 from *Saccharomyces cerevisiae* requires Zn(II) or Cd(II) for specific recognition of the UAS_G sequence (Pan & Coleman, 1989). An N-terminal fragment consisting of the first 63 amino acid residues of GAL4 [GAL4(63)] has been obtained by partial tryptic proteolysis of a cloned and overproduced N-terminal domain of 149 residues, GAL(149*). We show that GAL4(63) contains the minimal GAL4 DNA binding domain. GAL4(63) binds tightly 1-2 mol of Zn(II) or 2 mol of Cd(II). ^{113}Cd NMR of ^{113}Cd(II)-substituted GAL4(63) reveals structural identity between the metal binding domains of GAL4(63) and that of the larger precursor GAL4(149*). ^{113}Cd(II) can be substituted for the Zn(II) in GAL4(63), and two ^{113}Cd NMR signals are observed at 706 and 669 ppm, both suggesting coordination of ^{113}Cd(II) to three or four $-S^-$ ligands. With the exception of the N-terminal methionine, the only sulfur-containing residues are the six highly conserved cysteines. High-resolution ^{1}H NMR of Zn(II)-GAL4(63) and Cd(II)-GAL4(63) show the two proteins to have almost identical conformations and to be present as monomers in solutions up to millimolar concentration. This leads us to postulate that GAL4 does not possess a TFIIIA-like "Zn-finger" but forms a binuclear metal cluster involving all six cysteines in a "cloverleaf"-like array. GAL4(63) contains about 60% α-helix, estimated from circular dichroism. Removal of the native Zn(II) causes substantial unfolding of the secondary structure. Unlike GAL4(149*), the resultant apoprotein is not induced to refold by readdition of Zn(II) at low concentrations.

The transcription factor GAL4 from *Saccharomyces cerevisiae* contains a sequence of Cys residues, $\underline{Cys}^{11}X_2\underline{Cys}^{14}X_6Cys^{21}X_6\underline{Cys}^{28}X_2\underline{Cys}^{31}X_6Cys^{38}$, within its N-terminal DNA binding domain (Keegan et al., 1986). Although a Zn(II) binding site involving four Cys (as underlined above), similar to the tetrahedral Zn(II) complex in the "Zn-fingers" of TFIIIA (Miller et al., 1985), has been proposed (Johnston, 1987), all six Cys residues are highly conserved among several other transcription factors from yeast. Other transcription factors from eukaryotic organisms, e.g., the steroid receptors, also contain similar clusters of Cys residues [Evans and Hollenberg (1988) and references cited therein]. It has been shown not only that the mutations of the four putative Cys ligands affect DNA binding but also that a $Cys^{38} \rightarrow Gly^{38}$ mutant is deficient in specific DNA binding (Johnston & Dover, 1987, 1988). Although a Cys^{21} mutation has not been reported to date, it is possible that this particular cysteine could also function as a ligand.

We have shown previously (Pan & Coleman, 1989) that a polypeptide consisting of the N-terminal 147 amino acids of GAL4 plus two additional amino acids at the C-terminus from the cloning vector [denoted GAL4(149*)],[1] overexpressed and purified from *Escherichia coli*, incorporates 1.0-1.5 mol of Zn(II). Zn(II) can be reversibly removed from GAL4(149*) accompanied by a total loss of specific DNA binding affinity. Zn(II) can be substituted by Cd(II) with complete restoration of DNA binding properties. ^{113}Cd NMR of the latter protein shows the protein to contain two ^{113}Cd binding sites. The chemical shifts of the two bound ^{113}Cd(II), 707 and 669 ppm, suggest that each is ligated to at least three sulfurs (Pan &

† This work was supported by NIH Grants DK09070 and GM21919. The 500-MHz NMR was supported by NIH Grant RR03475, NSF Grant DMB-8610557, and ACS Grant RD259.
* Corresponding author.
‡ This work is in partial fulfillment of the requirements for the Ph.D.

[1] Abbreviations: GAL4(149*), cloned polypeptide fragment of the GAL4 transcription factor from yeast containing the N-terminal 147 amino acid residues plus 2 from the cloning vector; GAL4(63), tryptic fragment of GAL4(149*) containing the N-terminal 63 amino acid residues; GAL4(62*), cloned polypeptide fragment of GAL4 containing the N-terminal 61 amino acid residues plus 1 from the cloning vector; NMR, nuclear magnetic resonance; COSY, two-dimensional correlated spectroscopy; CD, circular dichroism; UAS_G, DNA sequence known as the upstream activation sequence specific for genes of the galactose operon; DIPF, diisopropyl fluorophosphate; TSP, sodium (trimethylsilyl)tetradeuteriopropionate.

0006-2960/90/0429-3023$02.50/0